

[Click here to view linked References](#)

The Synthesis of Hydroxyapatite from Artificially Grown *Red Sea Hydrozoan* Coral for Antimicrobial Drug Delivery System Applications

Ipek Karacan^{1*}, Nathan Cox², Annette Dowd², Razi Vago³, Bruce Milthorpe¹, Sophie Cazalbou⁴, and Besim Ben-Nissan¹

¹Faculty of Science School of Life Sciences, University of Technology, Sydney Australia

²Faculty of Science School of Mathematics and Physical Sciences, University of Technology, Sydney Australia

³Avram and Stella Goldstein-Goren Department of Biotechnology Engineering, Faculty of Engineering Sciences, Ben-Gurion University of the Negev, Beer Sheva, Israel

⁴CIRIMAT Carnot Institute, CNRS-INPT-UPS, Faculty of Pharmacie, University of Toulouse, France

*Corresponding author: ipek.karacan@gmail.com, <https://orcid.org/0000-0003-3110-4083>

Abstract

The Hydrozoan Millepora Dichotoma (MD) is a typical Red Sea species containing a porous skeleton in the form of aragonite crystalline calcium carbonate. Due to environmental considerations, the artificial production of coralline species under controlled conditions is pertinent and underway. Artificially grown MD was used as a raw material for the production of calcium phosphate, mainly hydroxyapatite bioceramics, to be used in the drug delivery systems as a drug carrier or in the tissue engineering such as bone graft. DTA-TGA, XRD, FT-IR, Raman, and SEM analysis were carried out to analyze both unconverted and converted artificial corals. Hydrothermally converted coral fine powders were loaded with Gentamicin (Gm) antibiotic, and the drug loaded particles were analyzed by SEM. Unconverted coral was mainly aragonite, while hydrothermally treated coral was completely converted to hydroxyapatite. Hydrothermally treated coral was showing agglomerated nodules up to 1 μm size consisting of nano-crystalline hydroxyapatite platelets in the size range of less than 100 nm. The general macropore size of the coral was found to be appropriate for osteoid growth, which is 100 to 600 μm range. These artificially grown corals can be easily produced and used for bone growth and repair and other biomedical applications.

Keywords:

Artificial Coral, *Millepora Dichotoma*, Hydrothermal Conversion, Hydroxyapatite

1. Introduction

Bone tissue engineering is the area that includes bone replacement due to bone tumors, maxillofacial, dental, and orthopedic clinical applications. Trauma, abnormal development, aging, tumors, and disease-related skeletal failures have been treated by surgical repairs or replacements to improve the quality of life.

1 During the last four or five decades, the number of skeletal deficiencies due to various socio-economic reasons
2 has been steadily increasing. Hence researchers globally have been working to find effective ways for
3 enhancement of bone formation and replacement via appropriate methods, designs, and biomaterials. Globally,
4 orthopedic and dental applications reflect nearly 55% of the total biomaterials market. Various biomaterials such
5 as synthetic and natural, including polymers, ceramics, animal and marine-derived natural ceramics and
6 composites have been developed as a substitute as implants or restore bone tissues [1-4].
7
8

9 One of the most appropriate materials for bone graft and implant applications is hydroxyapatite (HA), which is a
10 calcium phosphate bioceramic. HA is due to its crystalline structure and chemical composition, which is similar
11 to human bone. HA $[Ca_{10}(PO_4)_6(OH)_2]$ has been reported as a bone substitute material in various clinical and
12 therapeutic applications [5,6].
13
14

15 The use of porous HA has increased commercially during the last 30 years in clinical applications due to several
16 factors, which include porosity, available amount, size and interconnectivity crystalline structure, mechanical
17 integrity, slow biodegradability, which matches with tissue growth after implantation, and good
18 biocompatibility with both soft and hard tissues. It also provides good osteoconductivity and bioactivity that
19 supports cellular adhesion, proliferation, and differentiation of the mesenchymal stem cells (MSCs) and other
20 cell types [7,8].
21
22

23 Recently, a number of biomimetic synthesis methods have been introduced from the natural sources for the
24 synthesis of HA. These natural materials include marine structures such as coral, seashells, mussels, and algae,
25 which have been investigated by many groups for biomedical applications [9,10].
26
27

28 In comparison to synthetic ceramic materials, natural coral structures have been relatively more successful
29 for bone graft applications because of their unique interconnected porous structures and architecture that
30 allow vascularization. As stated earlier, the porosity range, which is between 100 to 500 μm , is similar to
31 the morphology of human cancellous bone [11].
32
33

34 The pore sizes and their interconnectivity are two of the most important factors for hard tissue growth. It
35 has been shown that its unique and uniform network system of channels can provide appropriate bone
36 regeneration and repair in clinical applications [5,12].
37
38

39 In addition to the improvement of hard tissue growth, the porous structure of the coral can be used for
40 various drug delivery systems such as antibiotics, bone regeneration drugs, or various minerals in order to
41 control release through the system [13,14]. However, the natural form of coral, whose chemical
42 composition is calcium carbonate ($CaCO_3$), is unsuitable for long-term implantation systems, specifically
43 for long bone applications because its dissolution rate is higher than other required bone growth rates [1].
44
45

46 In order to improve the biomaterial properties, the porous calcium carbonate exoskeleton structure of marine
47 invertebrates can be replaced with phosphatic material by various types of conversion methods. Hydrothermal
48 and other methods may be used to convert calcium carbonate to hydroxyapatite. The reason for the conversion
49 is that HA is harder than any form of $CaCO_3$, either aragonite or calcite. Most importantly, HA has much slower
50 dissolution rates dependent on the particle sizes used [4]. Marine invertebrates derived HA bioceramics can be
51 used as a drug carrier for the slow and controlled drug delivery systems due to its slower dissolution rate.
52
53
54
55
56
57
58
59
60
61
62
63
64
65

1 Therefore, Karacan *et al.* (2019) reported that coral derived HA was used as an antibiotic carrier in
2 biodegradable poly-lactic acid thin film implant coating to inhibit surgery-related infections [15].

3 The conversion method required, such as chemical, hydrothermal or mechanochemical, is determined by the
4 type of the coral species used, solid piece or powder or granulated form required, and also the type of the
5 calcium phosphate composition, which determines the solubility rate within the physiological environment [4].
6 During the hydrothermal process, the marine structure is converted to hydroxyapatite or tricalcium phosphate in
7 the presence of phosphate under high pressure and temperature. While the calcium carbonate is supplied from
8 either synthetic materials or natural animal or marine sources (such as coral and shells), the phosphate is
9 supplied from di-ammonium hydrogen phosphate [9,16,4]. Recently it was reported that *Halimeda spp.*
10 Calcified algae whose skeleton has calcium carbonate skeleton can be converted to HA by the same method
11 [17].
12
13
14
15
16

17 Marine structure conversion by hydrothermal or chemical methods has been reported by various groups. In
18 Australia, Ben-Nissan and his co-workers [9,1,10,18] reported that *Porites* and other corals and marine shells
19 were converted to HA successfully via the hydrothermal conversion method for medical usage.
20
21
22

23 Although the marine-based sources, especially corals, are highly attractive materials for the medical
24 applications, possible future high demand for commercial use can cause a negative effect on marine life and the
25 environment if the alive coral is sacrificed. Hence artificial ponds, containers, and laboratory-based systems
26 have been developed under controlled specific conditions for artificial coral growth [19]. Abramovitch-Gottlieb
27 *et al.* (2002) reported that the high-resolution computerized tank system was developed to grow colonies of
28 coral *Stylophora Pistillata* and the hydrocoral *Millepora Dichotoma* [19]. These artificial systems can provide a
29 30 cm per year growth rate of the artificial coral [19,20].
30
31
32
33

34 The MD, which is a Red Sea coral, is a species of hydrozoan, a coral comprised of polyps and also one of the
35 main contributors to skeletal calcium carbonate in reefs. The species is found predominately in the Indo-Pacific
36 region, but its occurrence has been from a plethora of other regions in the world. This species is most abundant
37 in habitats with a depth of 15m or less, which is referred to as a shallow reef habitat, so generally inshore areas
38 and shallow offshore sites [20,21]. This Red Sea coral was artificially grown by Abramovitch-Gottlieb *et al.*
39 (2002) for this current work [19]. We specifically used MD coral in Beer -Sheva, Israel at the University of Ben-
40 Gurion for the purpose of proving an important point that corals can be artificially grown under controlled
41 conditions for bone graft applications and drug delivery systems, without sacrificing the naturally grown corals.
42 Environmental issues as explained earlier is very real and protection of the natural coral by using this artificially
43 grown coral has great benefits to the society.
44
45
46
47
48
49

50 In this study, HA was synthesized with the hydrothermal treatment of artificial MD Red Sea coral in the
51 presence of di-ammonium hydrogen phosphate. Then, converted hydroxyapatite particles were loaded with
52 Gentamicin antibiotic (Gm) to be used as drug carriers. The characterization and morphology of this artificially
53 grown Red Sea coral before and after the conversion are reported.
54
55
56
57
58
59
60
61
62
63
64
65

2. Experimental

2.1. Preparation and Conversion Process

The MD was grown artificially in the Ben Gurion University of Negev, Israel, by Abramovitch-Gottlieb *et al.* (2002) and used for characterization prior and after conversion to HA [19].

The samples were cleaned with 2% sodium hypochlorite (bleach, NaClO) solution and ultra-pure water (18 milliQ) by the ultrasonic cleaner (UD80 SH-2L, Ultrasonics Pty. Ltd., Australia).

The cleaned coral skeleton is then crushed with an aluminum oxide ball mill at 46rpm and sieved in a 150 μm sieve before the conversion phase. This prepared powder then was converted to HA in a Parr hydrothermal reactor (Parr Instrument Company, USA) via a hydrothermal method with a temperature of 160-240 $^{\circ}\text{C}$ and a pressure of 1-3 MPa from 4 to 24 hours. The conversion time depends on the sample condition, such as powder or solid pieces, and its shape and size converted.

In this conversion process, based on our previous work, ammonium dihydrogen phosphate dibasic ($\text{NH}_4\text{H}_2\text{PO}_4$, 98%, Sigma Aldrich, Australia (phosphate) is used as a phosphate precursor [22,23,9].

During the hydrothermal process, the reaction involves [16].



2.2. Characterization

Simultaneous thermal analysis (STA) was utilized to analyze the thermal behavior of the cloned artificial Red Sea coral with which incorporates DTA-TGA (TG-DTA, SDT 2960, TA Instruments, New Castle, DE, US)

The sequence involved a nitrogen gas atmosphere at a flow rate of 150mL/min and a ramping temperature of 10 $^{\circ}\text{C}/\text{min}$, from 25 $^{\circ}\text{C}$ to 1100 $^{\circ}\text{C}$ with air cooling enabled. The alumina crucible is used during the analysis.

The microstructure and morphology of powders were determined by scanning electron microscope — (ZEISS Supra S5VP (Germany)) (SEM) with an operating voltage of 10 kV. The samples were cleaned by an ultrasonic cleaner in ethanol, dried, and coated with an approximately 10nm gold-palladium coating to eliminate charging.

Powder X-ray diffraction patterns were collected over the range 20 $^{\circ}$ to 80 $^{\circ}$ 2θ in 0.01 $^{\circ}$ intervals using CuK_α X-rays ($\lambda \sim 1.541 \text{ \AA}$) with Siemens D5000 X-ray Diffractometer (Germany).

Infrared measurements were performed on the powder form of unconverted and converted MD coral with a Thermo Fisher Scientific Fourier Transform infrared spectrometer (FTIR). Scans were collected over the range of 400 – 4000 cm^{-1} .

Raman characterization was carried out within a spectrometer range of 120-2000 cm^{-1} via Raman Spectrometer (Renishaw in Via Raman Microscope, Gloucestershire, UK) coupled with a Leica DMLB microscope (Wetzlar, Germany). The Wire 3.4 spectroscopic suite software and 785nm near-infrared diode laser were used, which is the ideal excitation wavelength for minerals, polymers, and standard material in addition to being a low energy wavelength reducing the risk of damage to the samples.

2.3. Drug Loading Study

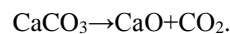
Gentamicin sulfate (Gm) (Sigma-Aldrich) was used as an antibiotic to process the drug loading method on the hydrothermally converted artificially grown MD coral. Gentamicin sulfate was dissolved into the 18 MQ ultra-pure water (MilliQ, Millipore, and Victoria, Australia). Artificial coral-based HA pieces and particles were immersed into the Gm solution, then they were placed in the ultrasonic cleaner (UD80 SH-2L, Ultrasonics Pty. Ltd., Australia) for 5min to allow the Gm solution to penetrate and coat the converted coral pores. Then, the HA pieces containing Gm solution were placed in the Rotary evaporator (John Morris Scientific, USA) at 60°C, 72 Mbar until and the liquid in the solution was evaporated. The samples than dried in a vacuum desiccator for 16h.

3. Results and Discussions

3.1. Thermal Analysis

The DTA-TGA trials were conducted under a custom sequence stated earlier.

In Fig 1, the DTA/TGA plot shows the thermal behavior of the artificial coral which clearly shows the conversion of calcium carbonate to calcium oxide and carbon dioxide between 600 and 800°C (770° C), with a reaction shown below:



The weight change and remaining weight in mg is a reduction of 41.38% (15.02mg) from the reaction happening to the finish. The diagram in Fig 1 is labeled according to weight loss over-temperature indicating specific points on the TG curve and reaction temperatures on DTA.

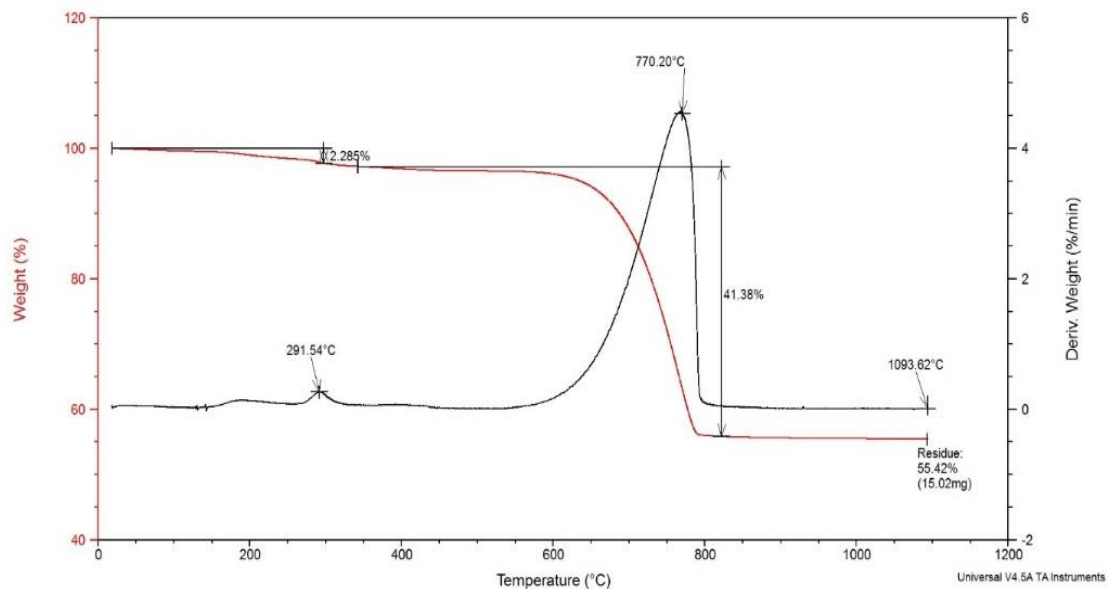


Fig 1. The DTA-TG diagram of *Millepora dichotoma* coral skeleton powder before conversion.

3.2. X-Ray Diffraction Analysis

XRD patterns of the cloned Red Sea coral skeleton before and after the hydrothermal conversion process are given in Fig 2. The main phases are aragonite (JCPDS 76-0606), and also a few minor peaks of calcite (JCPDS 05-0586) is observed. The XRD pattern, after the conversion, shows only the phase of HA (JCPDS 9-0432) in Fig 2-B. This pattern demonstrated high crystallinity and the absence of any free CaCO_3 confirming the completion of the reaction.

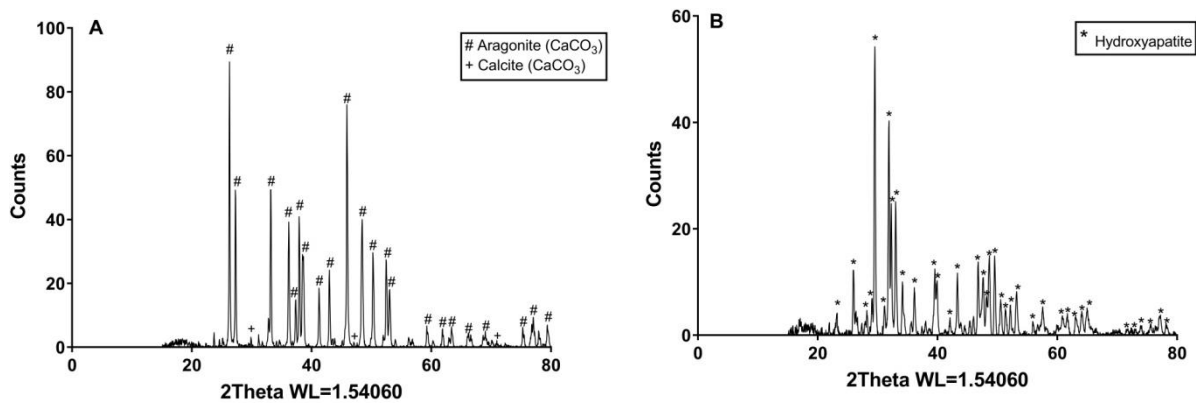
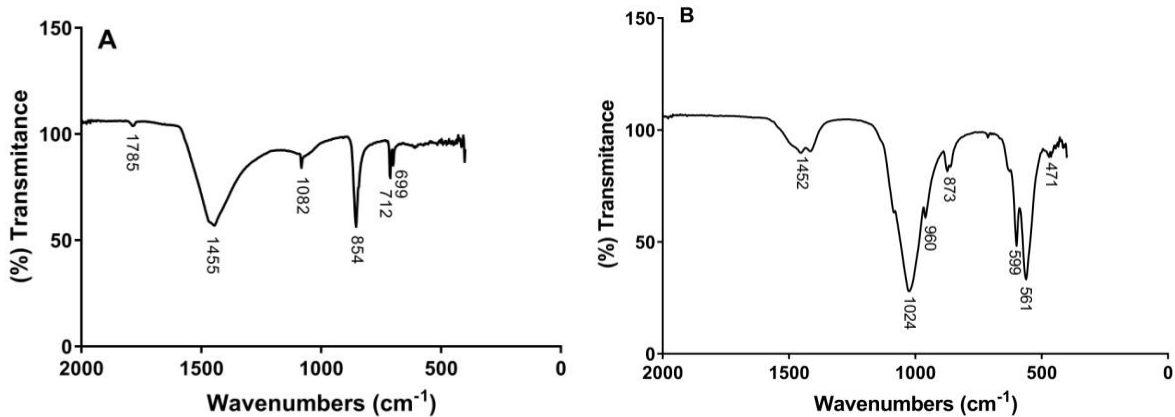


Fig 2. The XRD patterns of *Millepora dichotoma* Red Sea Coral before (A) and after (B) hydrothermal conversion process.

3.3. Fourier-transform infrared spectroscopy Analysis

The FT-IR analysis presents the mineral spectra of both the original coral and after its conversion to HA. According to the FT-IR spectra of unconverted coral (Fig 3-A), aragonite is a major phase, and calcite is undetected in the original coral structure. The ν_4 in-plane bending mode of the carbonate ion shows the characteristic doublet of aragonite at 699 cm^{-1} and 712 cm^{-1} . The ν_2 out of plane bending mode is seen at 854 cm^{-1} which is typical of aragonite, while the calcite ν_2 mode at 880 cm^{-1} is absent. The band at 1082 cm^{-1} is assigned to the $\nu_1(A'1)$ symmetric stretch of the carbonate ion. The ν_1 mode is infrared active in aragonite due to the site symmetry, but it is weak to inactive in calcite. The broad asymmetric band at 1455 cm^{-1} is assigned to the ν_3 antisymmetric stretch mode of carbonate in aragonite, and there is no peak evident at 1430 cm^{-1} due to the ν_3 mode in calcite. The weak band at 1785 cm^{-1} is a sum peak ($\nu_1 + \nu_4$).

The FT-IR spectra of the converted coral powder are given in Fig 2-B. The phosphate bands of HA are assigned as follows: 471 cm^{-1} (ν_2 bend), 561 cm^{-1} and 559 cm^{-1} (ν_4 bend), 960 cm^{-1} (ν_1 symmetric stretch), 1024 cm^{-1} (ν_3 antisymmetric stretch). Bands at 873 cm^{-1} and 1452 cm^{-1} correspond to ν_2 and ν_3 modes of carbonate ion substituted for the phosphate in HA [24]. It is plausible that this substitution creates patches of minute amounts of carbonate apatite within the bulk HA. Carbonate apatite has been observed in previous hydrothermal conversions.



3.4. Raman-Spectroscopy Analysis

According to Raman spectra of the unconverted coral skeleton (Fig 4-A), the most intense carbonate band is the symmetric stretch mode (ν_1) at a wavenumber of 1086 cm^{-1} which is insensitive to the polymorph. The smaller peak at 704 cm^{-1} is characteristic of the internal in-plane antisymmetric bend (ν_4) in aragonite. In contrast, a peak at 712 cm^{-1} corresponding to the ν_4 mode in calcite is absent (see database [25]). External lattice modes of aragonite are seen at 153 cm^{-1} and 206 cm^{-1} , but the diagnostic mode in calcite at 281 cm^{-1} is weak.

The Raman spectra of the coral sample after hydrothermal conversion, which is in Fig 4-B, presents the one strong major peak at 962 cm^{-1} corresponding to symmetric stretching (ν_1) of the phosphate group. Other

Fig 3. The FT-IR graphs of *Millepora Dichotoma* coral skeleton before (A) and after (B) hydrothermal conversion process.

phosphate bands at 432 cm^{-1} (ν_2 symmetric bend), 587 cm^{-1} (ν_4 bend), and 1046 cm^{-1} (ν_3 asymmetric stretch) indicate that the sample is predominantly HA. The minor carbonate band is observed at a wavenumber of 1072 cm^{-1} , which is indicative of minor carbonate apatite. As earlier shown in XRD results, no calcite was observed in fully converted coral.

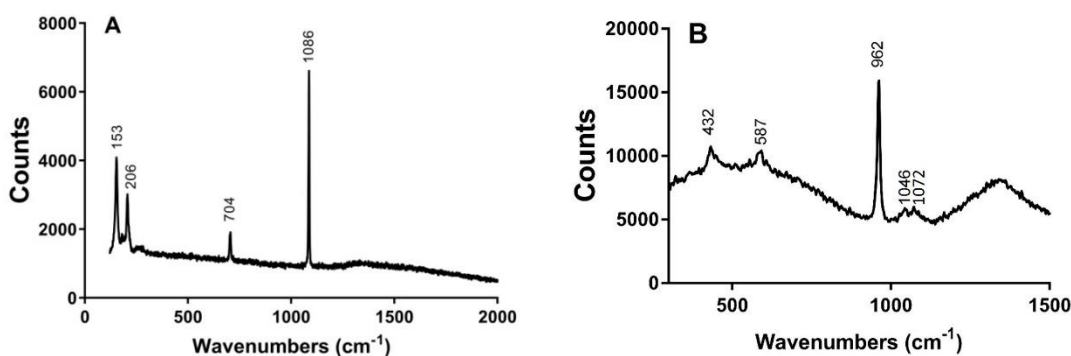


Fig 4. The RAMAN spectra of *Millepora Dichotoma* coral skeleton before (A) and after (B) hydrothermal conversion process.

3.5. Scanning Electron Microscope Analysis

Scanning electron microscope analysis was carried out on the cloned artificial *Millepora Dichotoma* coral skeleton in order to observe the surface morphology and its unique porous architecture in both before and after the hydrothermal conversion process. In Fig 5 to Fig 7, the surface structure of artificially grown *Millepora Dichotoma* is shown at low and high magnifications, which have both large pores and nano and mesopores in between the large pores and in spine areas.

Fig 5 also shows the differences in the pore sizes from the center to its surface and their interconnectivity. Additionally, somehow the interconnectivity is different in the center section, and its visual density is much less. This surprisingly, although not in the same size or density, it replicates the long bone structure in a primitive way.

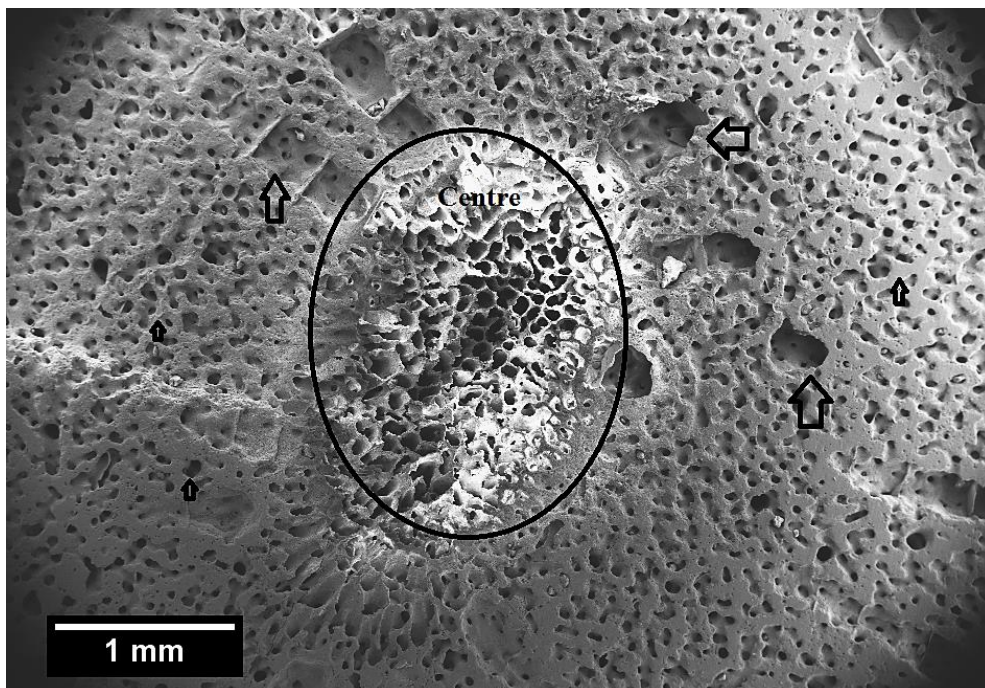
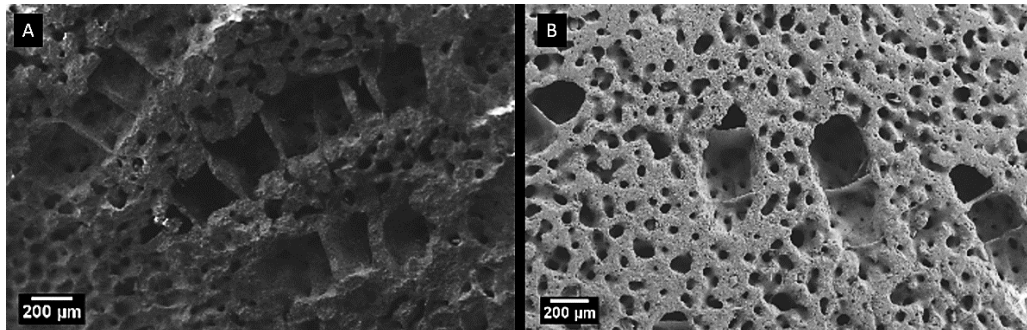


Fig 5. The inner structure of the skeleton of *Millepora Dichotoma* at low magnification, showing the porous structure in both outer and inner layers.

Fig 6 shows the comparison between the microstructure of the coral samples before (Fig 6-A) and after (Fig 6-B) conversion. The size of small pores in this section is approximately 40-60 μm , and large pores are around 200-250 μm . It shows that conversion has not changed the micro-pores sizes or shapes.

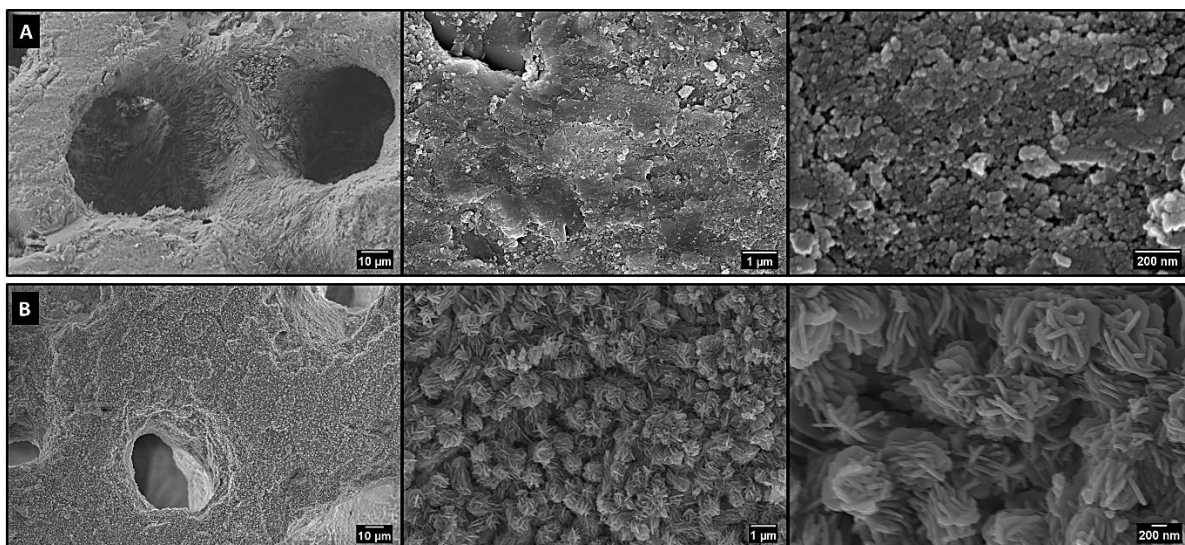
The pore size plays an important role in the structural integrity of bone scaffolds [26]. Cunningham *et al.* (2010) indicate a pore size between 40-100 μm is ideal for osteoid growth, which fits the pore width of not only the thin-walled pores but the thick ones also, therefore the resultant pores from the conversion favor osteoid growth. However, the well-established clinical work shows that for full vascularization, pore sizes of 100 to 500 μm range is required [27].

1 Therefore, this converted Red Sea coral after conversion presents a bioceramic material with a broad range of
2 different pore sizes, each unique providing possibilities for bone growth and repair. On the other hand, the
3 unconverted coral will not have the stiffness and strength required during bone regrowth due to its high
4 dissolution rate.
5



18 **Fig 6.** The SEM images of *Millepora Dichotoma* coral skeleton before (A) and after (B) hydrothermal
19 conversion process.
20
21

22 In Fig 7, the micro and mesostructure of the MD coral exhibit differences in the coral sample before (A) and
23 after (B) conversion. Fig 7-A represents the microporous structure of the coral as a first image at low
24 magnification. Therefore, the following images show the spherical- round shape CaCO_3 particles, which were
25 found to be agglomerated around the porous structure at high magnifications. On the other hand, Fig 7-B shows
26 the microporous structure of the MD coral after conversion in the first image at low magnification. In the
27 following two figures, after the conversion, coralline HA particles were observed as crystalline HA plate-like
28 particles in the range of 200-300 nm. The plate-like HA particles are much more evident at higher magnification
29 images. Although micro pores are not influenced by the conversion, it modifies the nano and mesostructure to
30 produce a very fine hydroxyapatite structure.
31
32
33
34
35
36
37



57 **Fig 7.** The SEM images of the *Millepora Dichotoma* coral skeleton before (A) and after (B) conversion at high
58 and low magnifications showing smaller pores between the HA agglomerated nodules consisting of smaller
59 plates.
60
61
62
63
64
65

3.6. Drug Loading Study

After the drug loading, the surface structure of coralline HA pieces was investigated with SEM. It was observed that Gm antibiotic solution evenly coats the surfaces of HA pieces as shown in Fig 8 at low and high magnifications. Although meso and nano-size porous on the HA plate-like particles were covered with the Gm layer, micropores are still observed on the coralline HA.

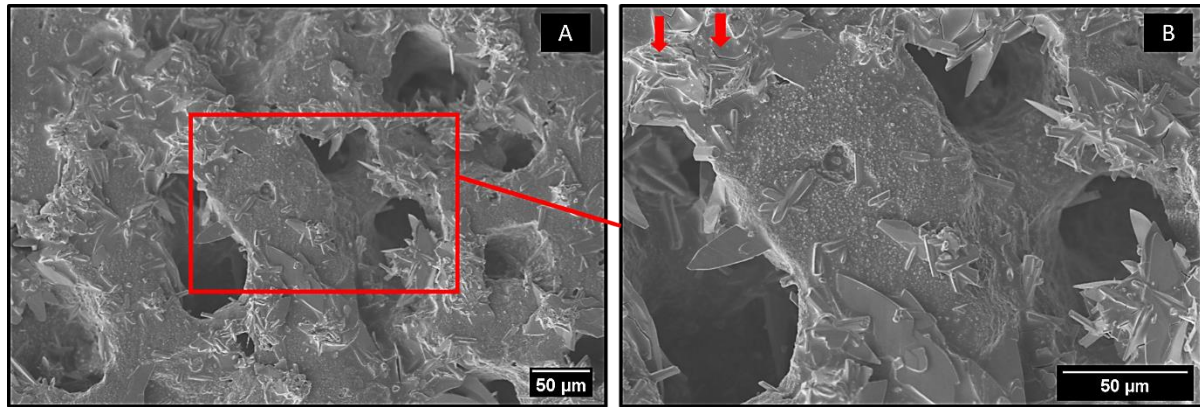


Fig 8. The surface of the coralline HA piece after Gm drug loading at low (A) and high (B) magnifications.

4. Concluding Remarks

The main aim of this study was to characterize and analyze the artificially grown Red Sea coral grown in controlled conditions. A high-resolution computerized tank system was developed that was used to grow colonies of the hydrocoral *Millepora Dichotoma* [20].

This artificially grown coral was used to produce calcium phosphate-based bioceramic (hydroxyapatite, HA) for medical applications such as bone graft and drug delivery systems. Due to environmental concerns, this artificial growth coral alternative was introduced. The growth rates were high as 30 cm per year.

The environmental problems are real and, unfortunately, are introduced by natural disasters or climate change and, more recently, by human-induced contaminations such as agricultural herbicides.

In addition to preventing the destruction of reef coral, this artificial production of corals provides a very efficient, standardizable and appropriate alternative for their potential medical use.

In this work, the conversion from artificial coral to HA was successfully carried out by using the hydrothermal method.

Different types of characterization methods were carried out, which included DTA-TGA, XRD, FT-IR, Raman, and SEM. Unconverted coral was mainly aragonite, while converted coral was HA with a minor amount of carbonate apatite. The same trend of conversion and mechanisms were observed in our previous work with natural *Goniopora* from the Great Barrier Reef. However, some morphological differences in their structure were observed due to the different species used.

SEM results show that after the conversion the structure of the *Millepora Dichotoma* coral has both large and small pores as micro, nano, and mesopores within their structure. The pore size of the coral was found to be quite an appropriate size for osteoid growth, which can be utilized in bone graft applications. Additionally, because of its nano and mesoporous structure, it can also be used for localized slow drug delivery applications.

Finally, the drug loading results show that the Gm drug loading process covers the nano and mesoporous structure on the HA particles as a uniform coating. Although, interconnected microporous structure on the coralline HA pieces still remained intact which can assist in the osteointegration after implantation. In addition, this drug delivery system can be useful for bone graft applications because of its interconnected micro-porous structure. Most importantly it is envisaged that it can be used as a drug delivery system in order to inhibit insertion in surgery-related infections via Gentamicin release to the surgical area.

To our knowledge, this is the first paper published on the characterization of this specific coral grown in the laboratory for medical applications. As a next step, *in vitro* cell culture studies on artificial MD coral have been examined and the results will be reported in due time. However, the morphology and the chemical composition is very similar to the original naturally collected coralline material. It is envisaged that future *in vitro* and *in vivo* studies will prove that point.

This work promotes the artificial cloning of coral species for both environmental reasons and the production of controlled high purity raw materials for biomedical applications.

Conflicts of interest

No potential conflict of interest was reported by the authors.

5. References

1. Ben-Nissan, B., Milev, A., Vago, R.: Morphology of sol–gel derived nano-coated coralline hydroxyapatite. *Biomaterials* **25**(20), 4971-4975 (2004). doi:<https://doi.org/10.1016/j.biomaterials.2004.02.006>
2. Heness, G.L., Ben-Nissan, B.: Innovative Bioceramics. *Materials Forum*. **27**, 104-114 (2004).
3. Senthil, R., Vedakumari, W., Sastry, T., Lee, J.: Hydroxyapatite and Demineralized Bone Matrix from Marine Food Waste – A Possible Bone Implant. *American Journal of Materials Synthesis and Processing*. **3**, 1-6 (2018). doi:10.11648/j.ajmsp.20180301.11
4. Tian, Q., Rivera-Castaneda, L., Dunn, Z.S., Liu, H.: Bioceramics for Orthopaedic Device Applications: Hydroxyapatite. In: Thian, E. S., Huang, J., Aizawa, M. (eds.) *Nanobioceramics for Healthcare Applications*. pp. 49-77. World Scientific (2017)
5. Choi, A.H., Ben-Nissan, B., Bendavid, A.: Thin Films and Nanocoatings of Hydroxyapatite on Titanium Implants: Production Methods and Adhesion Testing. LAP LAMBERT Academic Publishing, (2017)
6. Rodríguez-Lugo, V., Salinas-Rodríguez, E., Vázquez, R.A., Alemán, K., Rivera, A.L.: Hydroxyapatite synthesis from a starfish and β -tricalcium phosphate using a hydrothermal method. *RSC Advances* **7**(13), 7631-7639 (2017). doi:10.1039/C6RA26907A
7. Poinern, G.E.J., Brundavanam, R.K., Thi Le, X., Nicholls, P.K., Cake, M.A., Fawcett, D.: The synthesis, characterisation and *in vivo* study of a bioceramic for potential tissue regeneration applications. *Scientific Reports* **4**(1), 6235 (2014). doi:10.1038/srep06235
8. Pokhrel, S.: Hydroxyapatite: Preparation, Properties and Its Biomedical Applications. *Advances in Chemical Engineering and Science* **08**, 225-240 (2018). doi:10.4236/aces.2018.84016
9. Ben-Nissan, B.: Natural bioceramics: from coral to bone and beyond. *Current Opinion in Solid State and Materials Science* **7**(4), 283-288 (2003). doi:<https://doi.org/10.1016/j.cossms.2003.10.001>
10. Macha, I.J., Ozyegin, L., Chou, J., Samur, R., Oktar, F., Ben-Nissan, B.: An alternative synthesis method for di calcium phosphate (monetite) powders from mediterranean mussel (*mytilus galloprovincialis*) shells. *Journal of the Australian Ceramic Society* **49**, 122-128 (2013).

11. Kühne, J.-H., Bartl, R., Frisch, B., Hammer, C., Jansson, V., Zimmer, M.: Bone formation in coralline hydroxyapatite: Effects of pore size studied in rabbits. *Acta Orthopaedica Scandinavica* **65**(3), 246-252 (1994). doi:10.3109/17453679408995448
12. Elsinger, E.C., Leal, L.: Coralline hydroxyapatite bone graft substitutes. *The Journal of Foot and Ankle Surgery* **35**(5), 396-399 (1996). doi:https://doi.org/10.1016/S1067-2516(96)80058-5
13. Chou, J., Hao, J., Ben-Nissan, B., Milthorpe, B., Otsuka, M.: Coral Exoskeletons as a Precursor Material for the Development of a Calcium Phosphate Drug Delivery System for Bone Tissue Engineering. *Biological & pharmaceutical bulletin* **36**, 1662-1665 (2013). doi:10.1248/bpb.b13-00425
14. Karacan, I., Ben-Nissan, B., Sinutok, S.: Marine-Based Calcium Phosphates from Hard Coral and Calcified Algae for Biomedical Applications. In: Choi, A. H., Ben-Nissan, B. (eds.) *Marine-Derived Biomaterials for Tissue Engineering Applications*. Springer Series in Biomaterials Science and Engineering, pp. 137-153. Springer (2019)
15. Karacan, I., Ben-Nissan, B., Wang, H.A., Juritza, A., Swain, M.V., Müller, W.H., Chou, J., Stamboulis, A., Macha, I.J., Taraschi, V.: Mechanical testing of antimicrobial biocomposite coating on metallic medical implants as drug delivery system. *Materials Science and Engineering: C* **104**, 109757 (2019). doi:https://doi.org/10.1016/j.msec.2019.109757
16. Roy, D.M., Linnehan, S.K.: Hydroxyapatite formed from Coral Skeletal Carbonate by Hydrothermal Exchange. *Nature* **247**(5438), 220-222 (1974). doi:10.1038/247220a0
17. Choi, G., Karacan, I., Cazalbou, S., Evans, L., Sinutok, S., Ben-Nissan, B.: Conversion of calcified algae (*Halimeda* sp) and hard coral (*Porites* sp) to Hydroxyapatite. *Key Engineering Materials* **758 KEM**, 157-161 (2017). doi:10.4028/www.scientific.net/KEM.758.157
18. Karacan, I., Gunduz, O., Ozyegin, L.S., Gökce, H., Ben-Nissan, B., Akyol, S., Oktar, F.N.: The natural nano-bioceramic powder production from organ pipe red coral (*Tubipora musica*) by a simple chemical conversion method. *Journal of the Australian Ceramic Society* **54**(2), 317-329 (2018). doi:10.1007/s41779-017-0156-1
19. Abramovitch-Gottlib, L., Katoshevski, D., Vago, R.: A computerized tank system for studying the effect of temperature on calcification of reef organisms. *J Biochem Biophys Methods* **50**(2-3), 245-252 (2002). doi:10.1016/s0165-022x(01)00236-6
20. Green, D.W., Ben-Nissan, B., Yoon, K.S., Milthorpe, B., Jung, H.-S.: Natural and Synthetic Coral Biomineralization for Human Bone Revitalization. *Trends in Biotechnology* **35**(1), 43-54 (2017). doi:https://doi.org/10.1016/j.tibtech.2016.10.003
21. Meroz-Fine, E., Brickner, I., Loya, Y., Ilan, M.: The hydrozoan coral *Millepora dichotoma*: speciation or phenotypic plasticity? *Marine Biology* **143** (6), 1175-1183 (2003). doi:10.1007/s00227-003-1135-3
22. Ben-Nissan, B., Pezzotti, G.: Bioceramics Processing Routes and Mechanical Evaluation. *Journal of the Ceramic Society of Japan* **110**(7), 601-608 (2003).
23. Innes, J., Vago, R., Ben-Nissan, B.: Hydrothermal Conversion and Sol-Gel Coating of Red Sea Coral. *Key Engineering Materials* **240-242**, 43-46 (2003). doi:10.4028/www.scientific.net/KEM.240-242.43
24. Berzina-Cimdina, L., Borodajenko, N.: Research of Calcium Phosphates Using Fourier Transform Infrared Spectroscopy. In: Theophile, T. (eds.) *Infrared Spectroscopy: Materials Science, Engineering and Technology*, pp. 123-148. InTech (2012)
25. Lafuente, B., Downs, R.T., Yang, H., Stone, N.: The power of databases: The RRUFF project. In: *Highlights in Mineralogical Crystallography*. pp. 1-29. Walter de Gruyter GmbH (2015)
26. Cunningham, E., Dunne, N., Walker, G., Maggs, C., Wilcox, R., Buchanan, F.: Hydroxyapatite bone substitutes developed via replication of natural marine sponges. *Journal of Materials Science: Materials in Medicine* **21**(8), 2255-2261 (2010). doi:10.1007/s10856-009-3961-4
27. González Ocampo, J.I., Escobar Sierra, D.M., Ossa Orozco, C.P.: Porous bodies of hydroxyapatite produced by a combination of the gel-casting and polymer sponge methods. *Journal of Advanced Research* **7**(2), 297-304 (2016). doi:https://doi.org/10.1016/j.jare.2015.06.006